Automation of 3-dimensional cell culture in arrayed microfluidic devices

Sara I. Montanez-Sauri[1], **Kyung Eun Sung**[2], **John P. Puccinelli**[2], **Carolyn Pehlke**[2], and **David J. Beebe**[2],[*]

[1]Materials Science Program, University of Wisconsin-Madison

[2]Department of Biomedical Engineering and Wisconsin Institutes for Medical Research, University of Wisconsin-Madison

Abstract

The increasing interest in studying the interactions between cells and the extracellular matrix (ECM) has created a need for high throughput low cost three-dimensional (3D) culture systems. The recent development of tubeless microfluidics via passive pumping provides a high throughput microchannel culture platform compatible with existing high throughput infrastructures (e.g. automated liquid handlers). Here we build on a previously reported high throughput two-dimensional (2D) system to create a robust automated system for 3D culture. Operational controls including temperature and sample handling have been characterized and automated. Human mammary fibroblasts (HMFs) suspended in type-I collagen are loaded and cultured in microchannel arrays, and used to optimize the system operational parameters. A Peltier cooler maintains the collagen as a liquid at 4°C during cell seeding, followed by polymerization at 37°C. Optimization of this platform is discussed (e.g. controlling collagen contraction, increasing cell viability, preventing the removal of microchannel contents), and 3D distribution of HMFs is examined by fluorescent microscopy. Finally, we validate the platform by automating a previously developed 3D breast carcinoma co-culture assay. The platform allows more efficient 3D culture experiments and lays the foundation for high throughput studies of cell-ECM interactions.

Keywords

extracellular matrix; microfluidics; collagen; 3D; screening

Introduction

With recent advances in three-dimensional (3D) *in vitro* models, it is now widely accepted that the extracellular matrix (ECM) is one of the key regulators in various biological processes, including cancer progression [1–4] and stem cell differentiation [5]. Although cells can be maintained and grown using traditional flat, two-dimensional (2D) plastic substrates, studies have shown that cells grown in 3D conditions differ considerably in their morphology and differentiation [6], focal adhesion sites [7], gene expression profiles at the

[*]To whom correspondence may be addressed: Wisconsin Institutes for Medical Research, 1111 Highland Avenue, Room 6009, Madison, WI, USA, 53705, Tel: 1-608-262-2260, djbeebe@wisc.edu.

RNA level [8] and regulation of intracellular signaling [9] compared to cells grown in 2D conditions. These differences highlight the fact that 3D cell culture models mimic *in vivo* conditions better than 2D cell culture models, and provide enhanced interaction with neighboring cells as well as with ECM proteins [10, 11]. These results have created a need for higher throughput systems capable of screening the physical, chemical and biological properties of the 3D cellular microenvironment. However, adapting cell-based assays to high-throughput screening applications present challenges such as cell plating conditions, incubation times, compound addition parameters, and assay endpoint considerations that affect the quality of the final output [12]. As a result, microfabricated arrayed systems (e.g. cellular microarrays, microfluidic valved arrays, and tubeless microfluidic channel arrays) have been developed in attempts to provide a more reproducible and controllable high-throughput screening [13–15].

Cellular microarrays create spatially distributed cell-containing spots that are deposited on flat surfaces by robotic spotters to perform high-throughput analysis of cell-matrix, cell-cell interactions or toxicity screenings. Robotic spotting techniques possess the advantages of reducing the amount of materials needed for screening applications, providing a high degree of sample parallelization and facilitating the study of the material's influence on cellular behavior. For example, Flaim et al. patterned various ECM compositions on polyacrylamide-coated glass slides with a robotic spotter and placed cells on top of the spotted ECM proteins to examine the influence of the ECM composition on embryonic stem cell differentiation [16]. This method has also been employed to select biopolymers that induce a specific response in cells [17, 18], and to examine the combinatorial effect that different growth factors have on cell growth and differentiation [19]. Although cellular microarrays show promise for various screening applications, robotic spotting techniques have limitations such as the generation of satellite spots, inhomogeneous spots, misplaced or absent spots, and carryover of samples [20]. Khetani el al. used elastomeric stencils to culture human liver cells on micropatterns of type-I collagen, which overcame the previous limitation of patterning the surface of substrates using spotting techniques [21]. Additionally, Lee et al. spotted type-I collagen or alginate gels containing cells on a functionalized glass surface, which allowed culturing cells embedded in 3D instead of on top of ECM proteins [22]. However, since the entire patterned substrate is exposed to the same culture media, only one type of soluble stimuli can be applied at a time. Therefore, in cellular arrays, individual treatment of each spot is difficult and potential crosstalk between different spots can complicate interpretation of results.

Microfluidic valved arrays provide a different way of increasing the number of experimental conditions by allowing the incorporation of multiple fluids and cell types. In brief, microfluidic valved arrays typically consist of three different components (i.e., fluid channels (bottom), membrane valve (middle), and air channel (top)), in which the membrane valve deflects under air pressure applied through the air channel to control the opening of the fluid channel. The enclosed channel design enables the delivery of different soluble stimuli and limits crosstalk among different conditions in the system. For example, eight different soluble factors were incorporated in an 8 by 8 microfluidic array to examine the soluble factor effect in gene expression patterns of living cells [23], and to deliver two different cell types into designated chambers of a 6 by 6 microarray [24]. Moreover, microfluidic valved arrays are compatible with both 2D and 3D cell cultures to mimic *in vivo*-like environments [25, 26]. However, 3D cell culture is more difficult as the matrix can clog the network. Additionally, the need for complex connectors and pumps limits their adoption and widespread use.

Tubeless microfluidic channel arrays, operated by passive pumping [27], offer an alternative method of culturing cells that alleviates the limitations found in cellular microarrays and

microfluidic valved arrays, while facilitating the individualized treatment of microchannels with multiple soluble formulations [28]. Table 1 summarizes the functional advantages and limitations of traditional cell culture methods, microfabricated arrayed systems and tubeless microfluidic devices. Although tubeless microfluidic devices offer several important advantages for the screening of 3D cell cultures, one limitation is the relative separate loading process required for each microchannel. However, the loading process and all liquid exchanges are easily automated via existing liquid handlers addressing the arrayed microchannels. Samples are loaded into microchannels via surface-tension driven pumping called "passive pumping" [27]. The difference in surface tension created by placing different sized droplets on inlet and outlet ports results in an internal pressure differential, causing the fluid to be pumped from small drop (inlet) to the large drop (outlet). Therefore, the process only requires the use of a pipette to touch off drops on the ports' surfaces, and eliminates the need for external connectors, pumps or power amplifiers, enabling their incorporation into automated liquid handlers (ALH) [29]. Recently, a 192 polydimethylsiloxane (PDMS) microchannel array (MCA) and a single pipette ALH were operated for 2D cellular assays and tested for loading robustness, cell seeding consistency and staining quality. Each channel was addressed for 35 operations (dispensing and aspirating) for a typical cell-based assay, and a success rate higher than 99% was found over more than 30,000 times [30]. The system is compatible with 3D cell culture by passive pumping the cell-ECM mixture [31, 32]. However, automating 3D cell culture requires additional operational controls, such as temperature and sample handling [30].

In this work, we report the development of a robust automated microchannel platform for 3D cell culture. Type-I collagen is the major ECM protein component in connective tissues, and, accordingly, it was selected to support the 3D growth of cells. Human mammary fibroblasts (HMFs) are used for initial validation because of their susceptibility to the physical properties of type-I collagen, such as fiber diameter, alignment and stiffness [33]. HMFs are initially suspended in type-I collagen (1.3 mg/mL) and loaded with the automated platform into a 192-MCA. A Peltier cooler/heater maintains the 192-MCA at low temperature to keep type-I collagen as a liquid during the loading process. The collagen in the MCA is then polymerized at 37°C after the loading is complete. The platform is optimized to control collagen contraction, cell settlement, and prevent the removal of microchannel contents during washing. Moreover, the 3D distribution of cells was examined by fluorescent microscopy and their distribution along the microchannel length was quantified. Finally, we biologically validate the platform by automating a previously developed 3D breast carcinoma microfluidic co-culture model [34]. Breast carcinoma cell growth was analyzed after loading microchannels using the automated platform and similar results to those previously reported were obtained. Thus, the platform discussed in this paper lays the foundation for future 3D cell screening that can be used to study the interactions between cells and their ECM under specific conditions in a cost effective way.

Materials and Methods

Tubeless microfluidic device fabrication

Tubeless microfluidic devices composed of an array of 192 microchannels were fabricated using soft lithography techniques. Two layers of SU-8 100 (MicroChem, Newton, MA) were individually spun on a 6-inch silicon wafer and developed to create molded masters. The MCA layout was designed to conform to the dimensions of a standard 384 well plate. Poly(dimethylsiloxane) (PDMS, Sylgard 184 Silicon Elastomer Kit, Dow Corning Corporation, Midland, MI) was poured on top of the molded silicon wafer master, sandwiched between two transparency films under weight and cured at 80°C for four hours. The resulting MCA was then removed from the master mold, washed in 70% ethanol for sterilization purposes and air dried. After sterilization, the MCA was mounted on a culture-

treated polystyrene omnitray (Nunc, Rochester, NY). The PDMS microchannel array has overall dimensions of 111.0 mm long and 72.0 mm wide with a space of 4.5mm between each microchannel port (Figure 1A). Each microchannel (0.75mm wide, 0.25mm high, and 4.5mm long) has two ports (0.75mm input, 1.5mm output). The larger output port helped to maintain the larger radius of curvature for passive pumping (Figure 1B and C).

Cell culture and collagen gel preparation

The human mammary fibroblasts immortalized with human telomerase (HMFs; originally termed RMF/EG) were provided by Dr. Kuperwasser [35]. HMFs were cultured in flasks with high glucose (4.5mg/mL) Dulbecco's Modified Eagle's Medium (DMEM, #11995, Gibco, Grand Island, NY) supplemented with 10% calf serum and 1% penicillin/streptomycin (Invitrogen, Grand Island, NY) prior to use in the MCA. Flasks were maintained inside humidified incubators at 37°C containing 5% CO_2. In order to add cells to the MCA, cells were trypsinized (Gibco, Grand Island, NY), added to culture media, counted and spun down with a centrifuge at 1000 rpm for 3 minutes (5402, Eppendorf, Hamburg, Germany). At the same time, an acidic type-I collagen solution (3.92 mg/mL, rat tail, BD Biosciences, Bedford, MA) was neutralized with a solution of 100mM HEPES at a 1:1 ratio. This 100mM HEPES solution was previously prepared in 2X phosphate-buffered saline (PBS). DMEM was used to adjust type-I collagen concentration to 1.6 mg/mL. After mixing by pippeting up and down, cells were resuspended in DMEM at a density of 6×10^6 cells/mL. Finally, cells and the neutralized type-I collagen solution were mixed together to a final collagen concentration of 1.3 mg/mL and cell density of 6×10^5 cells/mL (approximately 700 cells/ microchannel). This collagen/cell mixture was added to two wells of a 96 well plate and placed in the automated platform. All collagen solutions were prepared by hand over ice to keep samples cold and avoid collagen polymerization.

Automated platform and components

An automated liquid handler (223 Sample Changer, 402 syringe pump and 250μL syringe, Gilson, Middleton, WI) was used to load microchannels, and a Peltier cooler/heater (242 Peltier rack, Gilson, Middleton, WI) was used to hold in place one 96 well plate and one microchannel array at the same time (Figure 1D). This Peltier cooler maintained a temperature of 4°C during cell seeding and ensured type-I collagen stayed as a liquid during sample loading.

Prior to using the ALH, the system was sterilized by spraying all ALH surfaces with 70% ethanol, rinsing the ALH probe (stainless steel, beveled shape tip, Gilson, Middleton, WI) and transfer tubing (Upchurch Scientific, Oak Harbor, WA) with 70% ethanol and treating all surfaces with UV light for 20 minutes. The Peltier cooler was then turned on and allowed to reach a stable temperature while the collagen samples were prepared by hand inside an aseptically prepared laminar flow hood. The 96 well plate containing the collagen/cell samples (BD labware, Franklin Lakes, NJ) and the 192 MCA were placed adjacently on the Peltier cooler (Figure 1D).

Automation of MCA pre-coating and cell seeding

All fluid manipulations on the 192 MCA were performed by the ALH. These manipulations are divided into three main processes that were run separately on different days. These processes are described in Figure 2 as 1) MCA pre-coating, 2) cell seeding and 3) cell staining. At the beginning of each of these processes the syringe probe was rinsed in cold water and sent to a touch off zone on the back of the ALH to prevent droplets from sticking to the end of the probe (step A). After rising, the probe moved to the 96 well plate to aspirate the solutions to be used in all three processes.

During Process 1 (MCA pre-coating), the ALH aspirated 40µL of the 50µg/mL type-I collagen solution from one well and dispensed 4µL to the input ports of 10 microchannels. These steps were repeated until a total of 80 microchannels were filled with collagen (steps A–C, purple square, Figure 2). After all channels were filled with the collagen solution in approximately 7 minutes, the MCA was kept overnight at 4°C until the next day.

The cell seeding process (Process 2) started on the next day and was divided into three separate loops (orange, magenta, and pink squares, Figure 2). The first loop rinsed the diluted collagen solution out and filled the microchannels with serum free (SF) media (DMEM, Gibco, Grand Island, NY). This was done by returning the MCA to the previously sterilized ALH along with the 96 well plate containing 4 wells filled with SF media. The ALH aspirated the SF media from the 96 well plate to treat 10 microchannels (step B, orange square), dispensed 4µL to the input ports (step C, orange square, Figure 2) and aspirated 2µL from the microchannel's output ports (step D, orange square, Figure 2). This first loop was repeated thirty two times in order to rinse 80 microchannels twice (orange square, Figure 2). Following this, a second loop was used to add DMEM droplets to the output ports of the microchannels (magenta square, Figure 2). In brief, the ALH probe aspirated 135µL of HMF culture media from one well of the 96 well plate (step E, magenta square) and dispensed 5µL to the output ports of approximately 27 microchannels (step F, magenta square, Figure 2). This loop was repeated a total of three times until 80 microchannels contained DMEM in their output ports (27, 27 and 26 microchannels treated in each loop). The media in the output ports served as a reservoir droplet for passive pumping the collagen/cell suspension that was added during the third loop (pink square, Figure 2) [27]. While the automated platform was performing the first and second loops, the collagen/cell suspension was prepared manually. After preparing the suspension, the MCA was ready for loading and 250µL of the collagen/cell suspension were added to two wells of a 96 well plate before running the third loop (pink square, Figure 2). Immediately after this, the ALH probe rinsed in water, went to the touch off zone (step A, pink square, Figure 2), and moved to one well containing the cell suspension, where the collagen/cell suspension was mixed twice at a flow rate of 0.5 mL/min (step G, pink square, Figure 2). Next, the probe aspirated 20µL of this cell suspension and added 4µL to the input ports of five microchannels in the MCA (step H, pink square, Figure 2). Adding the smaller droplet on the input port replaced the contents of the microchannels via passive pumping. After seeding five channels, the probe aspirated the residual volume that remained in the output ports, discarded this volume and rinsed (step I, pink square, Figure 2). This procedure was repeated a total of 16 times for seeding 80 microchannels in the MCA. After the loop was done, the MCA was kept on the cold Peltier for one minute, flipped upside-down and incubated at 37°C for two minutes. The MCA was then flipped every two minutes for a total of ten minutes to allow type-I collagen to polymerize and sustain cells in three dimensions. The total time required for each loop outlined in Figure 2 is summarized at the bottom of the figure with their corresponding colored loop codes.

Automation of viability assay – Cell staining

The viability of HMFs was assessed after the second day of culture in microchannels (LIVE/DEAD® Viability/Cytotoxicity Kit for mammalian cells, Invitrogen, Carlsbad, CA). Dyes solutions (4mM Calcein AM and 2mM Ethidium homodimer-1 in 1X PBS) were added to two wells of the 96-well plate (250µL each), and the plate was placed on the ALH platform.

This staining process consists of three main steps that were run consecutively one after the other (green, blue and light blue squares, Figure 2). The first loop includes a probe rinse in water (step A, green square), aspiration of the dyes solution from the reservoir wells and dispensing to the input ports of the microchannels (steps B–C, green square, Figure 2), an incubation period of ten minutes at room temperature (step D, green square, Figure 2), a

probe's rinse and touch off (second step A, green square, Figure 2) and a final aspiration of the excess dye from the output ports (step E, green square, Figure 2). At the second loop (blue square), the probe is rinsed in water again (step A, blue square), and a third loop follows in order to rinse microchannels with PBS a total of 3 times (steps F–I, light blue square, Figure 2).

Image acquisition and Analysis

Automated imaging for phase contrast and fluorescence was performed on an inverted microscope (IX70, Olympus, Center Valley, PA) and monochromatic camera (SPOT imaging, Diagnostic Instruments, Inc., Sterling Heights, MI) using x–y image acquisition journaling (MethaMorph 7.5, MDS Analytical Technologies, Downington, PA). A 4X objective was used to investigate the distribution of the cells within the microchannels and 10X was used for looking closer at the cell morphology. The distribution of cells along the length of microchannels was quantified by dividing microchannel images into 8 sections of 250µm with Image J software (Rasband, W.S., ImageJ, U.S. National Institutes of Health, Bethesda, Maryland, USA, http://rsb.info.nih.gov/ij/, 1997–2009) and counting the number of cells in each section. The viability of HMFs was calculated by counting the total number of live and dead cells in each microchannel. Three dimensional cell distributions were observed using a deconvolution microscope (IX71, Olympus, Center Valley, PA). Images were taken in the z direction using a 20X objective and a step size of 1µm to form 3D images using Slidebook 5.0 (Intelligent Imaging Innovations, Inc., Denver, CO). Images were deconvolved after their acquisition by applying nearest-neighbors parameters (theoretical spacing: 0.5um, substraction constant: 0.9). The 3D distribution of cells in the collagen matrix was evaluated by counting the total number of cells in the z direction using incremental steps of 25µm for a total of 250µm. Collagen fibers were observed using multiphoton laser scanning microscopy (MPLSM) and Second Harmonic Generation (SHG) with an excitation source produced by a Millenia 8W pump laser (Spectra Physics, Mountain View, Santa Clara, CA). Both systems were mounted around a Nikon Eclipse TE300 and images focused onto a Nikon 40X Plan Apo oil-immersion lens (NA=1.4) and SHG emission was observed at 445nm.

T47D breast carcinoma co-culture with HMFs

The human breast carcinoma T47D cell line T47D was obtained from Dr. M. Gould (University of Wisconsin, Madison). T47Ds were cultured in low glucose (1.0 mg/mL) DMEM (#11885, Gibco, Grand Island, NY) supplemented with 10% fetal bovine serum, and 1% penicillin/streptomycin (Invitrogen, Grand Island, NY) and HMFs were cultured with high glucose (4.5mg/mL) DMEM (#11995, Gibco, Grand Island, NY) supplemented with 10% calf serum and 1% penicillin/streptomycin (Invitrogen, Grand Island, NY) prior to use in the MCA. Both cell types were maintained at 37°C in a humidified atmosphere incubator containing 5% CO_2. For monoculture experiments, T47Ds were trypsinized, resuspended and added to neutralized type-I collagen to get a final collagen concentration of 1.3 mg/mL and cell density of 6×10^5 cells/mL (700 cells/microchannel). In co-culture experiments, T47Ds and HMFs were mixed in a 2:1 ratio in type-I collagen with DMEM used in HMF culture to get a final collagen concentration of 1.3 mg/mL and cell density of 4×10^5 T47Ds/mL (500 T47Ds/microchannel) and 2×10^5 HMFs/mL (250 HMFs/microchannel). The resulting T47D/collagen and T47DHMF/collagen mixtures were added to two different wells of a 96 well plate and placed in the automated platform. Samples were prepared by hand and over ice to avoid collagen polymerization.

T47D cell growth analysis

For the quantification of T47D cell growth, microchannels in the MCA were loaded with cells and type-I collagen using the automated platform. All other fluid manipulations were

performed with the automated platform using the optimized parameters described for the 3D culture of HMF cells. T47D cells were cultured for five days with media changes every other day. After the fifth day of culture, cells were fixed with 4% paraformaldehyde (PFA) for 20 minutes at room temperature and washed 3 times with PBS. Samples were further treated with 0.1M glycine in PBS to reduce the collagen autoflorescence, and the MCA was kept at 4°C overnight. The following day, the MCA was placed back on the automated platform and microchannels were washed 3 times with PBS and treated with 0.1% TritonX-100 in PBS for 90 minutes at room temperature to permeabilize cell membranes. Samples were then washed 3 times with PBS, and blocked with 10% goat serum overnight at 4°C. The next day, cells were stained and the MCA was incubated overnight at 4°C using primary antibodies diluted at a 1:50 (mouse monoclonal anti-human pancytokeratin, LabVision, Fremont, CA) and 1:150 dilution ratios (rabbit polyclonal anti-human vimentin, LabVision, Fremont, CA). Secondary antibodies were added the following day at a 1:150 dilution ratio (Alexa Fluor 594 goat anti-mouse; Alexa Fluor 488 goat anti-rabbit, Invitrogen, Carlsbad, CA) and incubated overnight at 4°C. For counterstaining the nuclei, Hoechst 33342 was used at 20µg/mL (H3570, Invitrogen, Carlsbad, CA). Lastly, microchannels were washed with PBS 4 times.

Analysis of the total T47D staining area per microchannel was done using two methods, fluorescence microscopy and fluorescence scanning (Typhoon Trio, GE Healthcare). Fluorescence microscopy images provided a standard for comparing the results from the scanner for validation. Fluorescence images were obtained for each microchannel using the x–y image acquisition journaling (MethaMorph 7.5) that was previously used for the viability analysis. Total T47D staining area was calculated using Image J software. For the automated analysis, the MCA was placed on the scanner, and software analysis was performed on the scanned image to analyze the total fluorescence intensity per microchannel (ImageQuant TL, Array version 7.0, GE). Samples with no primary antibody were used as negative controls. All analyses were conducted over the entire channel region.

Results and Discussion

The microfluidic platform described in this work was automated for 3D cell culture through the incorporation of a microchannel array and an ALH that performed all fluidic manipulations in the array. The Peltier device used in this platform maintained a low temperature during cell seeding, enabling the handling of collagen samples. Due to intrinsic characteristics of 3D culture, the successful automation of this 3D platform required a different set of optimized parameters from a previously reported 2D platform [30]. Specifically, the optimization of several operations and parameters such as surface treatment, sample mixing and total loading time was required in order to: 1) reduce collagen contraction, 2) maintain a uniform cell seeding distribution, 3) prevent the removal of contents in microchannels during sample washing, and 4) minimize the total time that cells spent on the platform. First, we discuss in more detail how we addressed each of these points. Second, we utilize biological validations to evaluate: 1) cell morphology, 2) cell viability, 3) distribution of cells in the 3D matrix, and 4) collagen fiber formation. Finally, we further validate the optimized platform as a screening tool via co-cultures of T47D breast carcinoma cells and human mammary fibroblasts in a type-I collagen matrix and comparing T47D cell growth with previously reported data [34, 36]. This co-culture experiment was completely automated by using the optimized operations and parameters discussed before to perform all fluidic manipulations including collagen surface coating, cell seeding, media changes, fixing, blocking, and inmmunostaining.

System Automation and Optimization of Operational Parameters

Collagen gel contraction was minimized in our 3D cell cultures by treating the interior surface of microchannels before adding the collagen/cell suspension. Controlling contraction is important in microchannels as it can reduce sample size significantly and make sample analysis more difficult. Therefore, in order to control the contraction in our microchannels, a type-I collagen monomer pre-coating step previously used [31] was automated and included before loading the collagen/cell suspension (Process 1, Figure 2). Serum free media was used to rinse out the collagen-monomer solution in order to keep the PDMS surface hydrophobic (Process 2, orange square, Figure 2). This was particularly important as proteins in serum containing media can make the PDMS surface hydrophilic and reduce the contact angle of the droplets necessary for passive pumping [27].

Seeding cells inside microchannels during Process 2 required mixing the collagen/cell suspension continuously in order to maintain a uniform cell seeding distribution along microchannels. In order to achieve this, the collagen/cell suspension in wells was mixed by pipetting with the automated probe after loading 5 channels in the MCA. Previously, magnetic stir bars were used inside wells to keep cell suspensions homogeneously mixed in 2D cell cultures. However, using stir bars required the incorporation of magnetic plates that are difficult to add in our platform due to the presence of Peltier devices that are required to keep collagen samples cold. Figure 3A shows a microchannel loaded with the automated platform. An even distribution of cells was observed along the length of the microchannel. This distribution of cells was further quantified in Figure 5B for different positions in the MCA. Therefore, pipetting the collagen/cell solution multiple times with the automated probe proved to be effective for mixing the solution and ensuring a uniform cell density along the MCA.

The aspiration of excess volumes is necessary when performing multiple washes as fluid is replaced from the input to output port via passive pumping and output drops increase in volume [27]. This fluid replacement is possible in 3D cell cultures due to contraction of the matrix on the top surface of the microchannel that permits fresh fluid to flow inside the microchannel [31]. However, the removal of excess volumes from the output ports in 3D cultures requires care so as not to accidentally remove any of the collagen/gel sample when aspirating the output droplets. In order to avoid removal of the channel contents during aspiration, the probe's height was modified in Process 3, such that during the excess volume aspiration steps (steps E and I, green and blue squares respectively, Figure 2) the probe was raised 1 mm higher than during the dispensing steps on the input ports (steps C and G, green and light blue squares respectively, Figure 2). Finally, two loops were included at the end of the Process 3 that ensured the dyes solution was rinsed out from the microchannels (steps A thru I, blue and light blue squares, Figure 2).

The total time that cells spent in each process on the automated platform was critical in order to maintain cell viability. This was particularly important in processes that involved either cells suspended in cold type-I collagen (pink square, Process 2, Figure 2) or cells cultured in microchannels (Process 3, Figure 2). Accordingly, Process 2 was divided into three loops that were run separately. The first and second loops (orange and magenta squares, Figure 2) were run during sample preparation, such that the pre-coating solution was rinsed out of microchannels (orange square, Figure 2), and output droplets were dispensed on the array for passive pumping (magenta square, Figure 2) before cells were suspended in type-I collagen and added to the 96 well plate. The bottom of Figure 2 shows a color code with the total time spent for each loop in all the three processes. The platform takes approximately 47 minutes to run all three loops in Process 2. However, by separating Process 2 into three separate loops, cells stayed in the cold collagen for only 22 minutes (pink square). It is important to note that although the automated platform was able to load

the MCA with the pre-coating solution in a shorter amount of time (Process 1, approximately 7 minutes), a continuous rinsing of the probe and mixing of the collagen/cell suspension during cell seeding was necessary in order to avoid clogging the probe and ensuring a uniform cell seeding density along the MCA. The total time required for staining cells with the automated platform (Process 3) was also important since cells are not fixed in viability assays, but rather stay alive during the staining process. Other staining protocols (e.g. immunostaining) require fixing the cells before staining and thus, the total time spent on each process after fixing is not critical. Nevertheless, a viability assay was found useful for testing the capability of the automated platform for staining cells and for determining the sensitivity of cells to previous fluidic manipulations (cell loading, cell mixing, cell seeding). The total time spent on Process 3 was shortened by adding droplets only to the input ports (steps C and G, green and light blue squares, Figure 2) and aspirating out the same volume from the output ports (steps E and I, green and blue squares, Figure 2), instead of aspirating droplets from output and input ports and dispensing new droplets to both input and output ports. Passive pumping was still possible due to the presence of media droplets on the output ports that were already present during cell culture.

Biological Validation of the Automated Platform

After optimizing the system's operational parameters, we examined the viability and morphology of HMFs seeded and cultured with the automated platform as compared to cells seeded in microchannels by hand. Figure 3B shows a microchannel that was loaded manually and Figure 3C a microchannel randomly chosen from a MCA loaded with the automated platform. As can be seen from the figures, HMFs show a similar stretched morphology for both loading techniques. Moreover, HMFs were seen in different focal planes (pointed out by white arrows) in microchannels loaded both by hand and with the automated platform, which suggested that cells were also distributed in the collagen matrix in 3D.

The viability of HMF cells was evaluated using several pipetting speeds and number of mixes (mixing up and down) in order to determine the optimum pipetting manipulation for the cell seeding process (Process 2, Figure 2). This is particularly important in our platform as the collagen/cell suspension needs to be continuously mixed to maintain a uniform cell seeding distribution in the MCA. However, a continuous and vigorous pipetting of the collagen/cell suspension can also cause cell damage. Excessive trituration (mixing via pipetting up and down) is known to produce shear stress and damage to embryo cultures [37]. In our system, cells are exposed to shear stresses during sample mixing, while type-I collagen is still a liquid. After the loading is finished and type-I collagen gel is polymerized, cells are embedded in 3D type-I collagen and exposure to shear stress is minimal for subsequent fluid changes. Therefore, pipetting triturations in our system were minimized during the cell seeding process (Process 2, Figure 2) to reduce shear stresses and possible damage to the cells. Speeds varying from 2 mL/min to 0.5 mL/min were tested and cell viability was assessed to look at how cells responded to the pipette's manipulation. It was found that a speed of 0.5 mL/min increased cell viability to 90% that contrasted with the initial cell viability of 31% found when using a speed of 2 mL/min (Figure 4A). In addition to the speed of pipetting, the total number of mixes also affected cell viability. Initially, the collagen/cell suspension was mixed at 0.5mL/min four times (pipetting up/down counting as one mix) before loading into the microchannels. Subsequently, it was found that reducing the number of mixes to two increased cell viability to 99% (Figure 4B). Thus, the optimum condition for mixing the collagen/cell sample was found to be mixing at the reduced speed of 0.5 mL/min twice after loading five microchannels in the array. A 99% in viability demonstrates that our platform is not just robust enough to aspirate and dispense a collagen/

cell suspension, but gentle enough to mix cells and keep them viable for cell culture purposes as well.

In order to corroborate the 3D distribution of cells inside microchannels, cells were stained using the protocol previously described with the automated platform and observed via fluorescent microscopy. Figure 4C shows a stack of images from a microchannel that was seeded, stained and washed using the automated platform. HMFs showed to be distributed along 200µm of matrix inside a 250µm high microchannel. Previously, a collagen contraction of approximately 16.5% (167.25µm in 200µm high microchannels) was reported for type-I collagen gels containing HMFs [31]. Although the actual height of the microchannels used in this work was 250µm, a contraction of 20% was observed, which is similar to the 16.5% collagen contraction reported previously.

After observing that cells were distributed along the length (Figure 3A) and height (Figure 4C) of microchannels, their distribution through the MCA was examined. Six microchannels were randomly selected to evaluate the capability of the automated platform for obtaining a uniform cell distribution along the length of microchannels (microchannels 1, 3 and 5) and a 3D cell distribution (microchannels 2, 4 and 6). As can be seen from Figure 5A, the automated platform was able to seed cells uniformly along the length and height of microchannels in different places in the MCA. This qualitative observation was further validated by quantifying the number of cells in 8 equally divided sections (250µm in length per section) along the channel length (Figure 5B). Cell number averages of 42±3, 45±2 and 45±1 were found every 250µm, in microchannels 1, 3 and 5, respectively. No significant differences were found between cell average numbers on these microchannels. Additionally, the three dimensional cell distribution was quantified for microchannels 2, 4 and 6 (Figure 5C). Cells were observed at heights starting from 17µm above the bottom of the microchannel (microchannel 4) to up to 231µm (microchannel 6). Finally, the cell viability was evaluated and found to be 90% along the whole MCA. These results confirm that our platform optimization was successful and that mixing the collagen/cell suspension and flipping the device after seeding cells was effective enough to seed cells uniformly along the length of microchannels and to suspend cells in 3D during matrix polymerization.

Finally, type-I collagen fiber formation was examined in order to determine if our platform was controlling collagen polymerization properly. It has been shown previously that type-I collagen polymerization in microsystems is different from macro systems mainly because of increased heat transfer caused by the high surface area to volume ratio of microsystems [31]. This high surface area to volume ratio accelerates sample warming and results in a faster polymerization in microsystems. In order to control for this, a cold Peltier device was used to keep collagen samples at low temperatures during sample loading. Second harmonic generation (SHG) imaging revealed that a similar type-I collagen fiber structure is obtained with microchannnels loaded from collagen samples kept on the Peltier device (Figure 6A–B) and microchahnels loaded with collagen samples kept over ice (Figure 6C). This similarity in type-I collagen fiber structure was also observed in microchannels loaded right before loading the MCA (0 minutes, Figure 6A) and right after loading the whole MCA (22 minutes, Figure 6B). Figure 6D shows that no significant differences in SHG intensities were observed in microchannels A thru C. This confirmed that our platform controls the temperature of the collagen/cells suspension in the wells and that a similar type-I collagen structure can be obtained in microchannels loaded between 0 to 22 minutes.

Screening of T47D cell growth

A 3D co-culture system of T47D breast carcinoma cells with HMFs was utilized to validate the screening capabilities of the automated platform. Previously, this model was used to study paracrine signaling pathways between T47D and HMFs in type-I collagen gels [36] and

showed that the presence of HMFs in T47D cultures induced an increase in T47D carcinoma cell growth when compared to T47D monocultures. More recently, this 3D model was validated for microfluidic cell culture [34]. Here we used the automated microfluidic platform to seed, fix and stain T47D breast carcinoma cells and HMFs inside tubeless microchannels. All fluidic manipulations were performed using the optimized parameters previously found for HMF cell culture. T47D cells were cultured in monocultures (T47D) and co-cultures (T47D and HMFs) for five days inside microchannels and T47D cells were distinguished from HMFs by immunocytochemical labeling of pancytokeratin (CK) in T47Ds and vimentin (VM) in HMFs. Figure 7A and 7B show images of microchannels containing monocultures of T47Ds and co-cultures with HMFs, respectively. As can be seen from the figures, T47Ds (red) grew in bigger clusters when co-cultured with HMFs (green) than in monocultures. In order to quantify this difference in T47D cluster size, the total CK-positive staining area was used as a surrogate of T47D growth. Previous models have shown that there is a direct correlation between T47D cell number and CK-positive area [34, 36]. We confirmed this observation in our system by counting the total number of T47D nuclei per clusters manually, and found that not only the CK-positive area correlates to cell number, but nuclei staining as well (Figure 7E). This last correlation can be particularly useful for performing a fast analysis of the total T47D cell number in monocultures and simplifying the staining protocol, as fixing and secondary staining are not necessary. Therefore, T47D cell growth was evaluated in monocultures and co-cultures using two methods. The first method quantified the total CK-positive fluorescence per microchannel by using a fluorescent scanner and the second method evaluated total T47D nuclei area in microchannels by manually adjusting a threshold of T47D clusters with Image J. Thus, the first method provided a fast automated analysis of total CK-staining area per microchannel, and the second method served as a comparison standard. Figures 7C and 7D show data obtained from the scanner and manual calculation, respectively. In both cases, cluster size of T47Ds was approximately 1.5 times bigger in co-cultures than in monocultures. This induction in T47D cells agrees with previous reports where a 1.5 to 2.5-fold increase in breast carcinoma cell growth was observed [34]. The fact that we were able to obtain similar results between the automated scanner and manual calculations shows that either CK-positive staining area or nuclei staining area can be used to quantify T47D cell number and that the scanner could be used as a tool for a faster analysis. These results also confirm the utility of the automated microfludic platform for 3D culture and promise to be a useful tool for other cell screenings.

Conclusion

The increased interest in studying cells in 3D has created a need for low cost higher throughput systems capable of screening for parameters in the microenvironment that influence cellular behavior. Tubeless microfluidic devices promise to be a useful tool for screening the cellular microenvironment due to their easy incorporation with automated liquid handlers and scanners, their capacity for treating samples individually, their ability to increase the number of replicates and experimental conditions, and their ability to markedly reduce reagent consumption and total costs. This work has shown that a tubeless 192-MCA can be easily incorporated into an automated liquid handler after system optimization for 3D cell culture. The individualized treatment allowed for the culture of T47D breast carcinoma cells in monocultures and co-cultures with human mammary fibroblasts in separate compartments. Differences in T47D cell growth in monocultures and co-cultures were quantified using a laser scanner for a rapid high throughput analysis and confirmed with manual calculations. Moreover, the total reagent volumes were significantly reduced when compared to traditional 3D cell culture methods. For example, one data point in a MCA only requires the loading of one microchannel with 2μL of sample, whereas a traditional 3D cell culture assay (e.g. 96 well plate) requires a minimum of 50μL. Therefore, a 25-fold in

savings can be obtained with microchannels when compared to traditional 3D culture methods. This is particularly important for high throughput 3D cell screenings that utilize numerous data points, primary cells and costly ECM proteins.

In addition to reducing total costs and effort, this automated platform was validated by looking at the cell morphology, cell viability, 3D distribution of cells and type-I collagen fiber structure in microchannels loaded with the automated platform. When the cells seeded by the automated platform where compared with cells cultured by hand, it was found that our automated platform was gentle enough to handle cells and no morphological differences were seen. The screening capabilities of this platform were further tested by loading human breast carcinoma cells (T47Ds) with human mammary fibroblasts and it was found that the platform was robust enough to co-culture these cells in microchannels. An automated scanning analysis was performed using this model and results similar to those reported elsewhere were obtained [34, 36]. In conclusion, the microfluidic platform presented in this work promises to be useful for future cell screenings that will facilitate the study of cell-ECM interactions.

Acknowledgments

References

1. Bissell MJ, Radisky D. Putting tumours in context. Nature Reviews Cancer. 2001; 1(1):46–54.

2. Debnath J, Brugge JS. Modelling glandular epithelial cancers in three-dimensional cultures. Nature Reviews Cancer. 2005; 5(9):675–688.

3. Sutherland RM, Sordat B, Bamat J, Gabbert H, Bourrat B, Muellerklieser W. OXYGENATION AND DIFFERENTIATION IN MULTICELLULAR SPHEROIDS OF HUMAN-COLON CARCINOMA. Cancer Research. 1986; 46(10):5320–5329. [PubMed: 3756881]

4. Wozniak MA, Desai R, Solski PA, Der CJ, Keely PJ. ROCK-generated contractility regulates breast epithelial cell differentiation in response to the physical properties of a three-dimensional collagen matrix. Journal of Cell Biology. 2003; 163(3):583–595. [PubMed: 14610060]

5. Grayson WL, Ma T, Bunnell B. Human mesenchymal stem cells tissue development in 3D PET matrices. Biotechnology Progress. 2004; 20(3):905–912. [PubMed: 15176898]

6. Petersen OW, Ronnovjessen L, Howlett AR, Bissell MJ. INTERACTION WITH BASEMENT-MEMBRANE SERVES TO RAPIDLY DISTINGUISH GROWTH AND DIFFERENTIATION PATTERN OF NORMAL AND MALIGNANT HUMAN BREAST EPITHELIAL-CELLS. Proceedings of the National Academy of Sciences of the United States of America. 1992; 89(19): 9064–9068. [PubMed: 1384042]

7. Cukierman E, Pankov R, Stevens DR, Yamada KM. Taking cell-matrix adhesions to the third dimension. Science. 2001; 294(5547):1708–1712. [PubMed: 11721053]

8. Nelson CM, Bissell MJ. Of extracellular matrix, scaffolds, and signaling: Tissue architecture regulates development, homeostasis, and cancer. Annual Review of Cell and Developmental Biology. 2006; 22:287–309.

9. Li S, Lao JM, Chen BPC, Li YS, Zhao YH, Chu J, Chen KD, Tsou TC, Peck K, Chien S. Genomic analysis of smooth muscle cells in three-dimensional collagen matrix. Faseb Journal. 2002; 16(13) 97-+.

10. Abbott A. Cell culture: Biology's new dimension. Nature. 2003; 424(6951):870–872. [PubMed: 12931155]

11. Birgersdotter A, Sandberg R, Ernberg I. Gene expression perturbation in vitro - A growing case for three-dimensional (3D) culture systems. Seminars in Cancer Biology. 2005; 15(5):405–412. [PubMed: 16055341]

12. Maddox CB, Rasmussen L, White EL. Adapting Cell-Based Assays to the High Throughput Screening Platform: Problems Encountered and Lessons Learned. JALA Charlottesv Va. 2008; 13(3):168–173. [PubMed: 19492073]

13. Puccinelli, JP.; Beebe, DJ. High Throughput Micofluidics for Biology. In: Tian, WC.; Finehout, EJ., editors. Microfluidics for Biological Applications. New York, NY: Springer Science and Business Media, LLC; 2008. p. 241-270.

14. Khademhosseini A, Langer R, Borenstein J, Vacanti JP. Microscale technologies for tissue engineering and biology. Proceedings of the National Academy of Sciences of the United States of America. 2006; 103(8):2480–2487. [PubMed: 16477028]

15. Maerkl SJ. Integration column: Microfluidic high-throughput screening. Integrative Biology. 2009; 1(1):19–29. [PubMed: 20023788]

16. Flaim CJ, Chien S, Bhatia SN. An extracellular matrix microarray for probing cellular differentiation. Nature Methods. 2005; 2(2):119–125. [PubMed: 15782209]

17. Yliperttula M, Chung BG, Navaladi A, Manbachi A, Urtti A. High-throughput screening of cell responses to biomaterials. European Journal of Pharmaceutical Sciences. 2008; 35(3):151–160. [PubMed: 18586092]

18. Anderson DG, Levenberg S, Langer R. Nanoliter-scale synthesis of arrayed biomaterials and application to human embryonic stem cells. Nature Biotechnology. 2004; 22(7):863–866.

19. Flaim CJ, Teng D, Chien S, Bhatia SN. Combinatorial signaling microenvironments for studying stem cell fate. Stem Cells and Development. 2008; 17(1):29–39. [PubMed: 18271698]

20. Hartmann M, Sjodahl J, Stjernstrom M, Redeby J, Joos T, Roeraade J. Non-contact protein microarray fabrication using a procedure based on liquid bridge formation. Analytical and Bioanalytical Chemistry. 2009; 393(2):591–598. [PubMed: 19023564]

21. Khetani SR, Bhatia SN. Microscale culture of human liver cells for drug development. Nature Biotechnology. 2008; 26(1):120–126.

22. Lee MY, Kumar RA, Sukumaran SM, Hogg MG, Clark DS, Dordick JS. Three-dimensional cellular microarray for high-throughput toxicology assays. Proceedings of the National Academy of Sciences of the United States of America. 2008; 105(1):59–63. [PubMed: 18160535]

23. King KR, Wang SH, Irimia D, Jayaraman A, Toner M, Yarmush ML. A high-throughput microfluidic real-time gene expression living cell array. Lab on a Chip. 2007; 7(1):77–85. [PubMed: 17180208]

24. Wang HY, Bao N, Lu C. A microfluidic cell array with individually addressable culture chambers. Biosensors & Bioelectronics. 2008; 24(4):613–617. [PubMed: 18635348]

25. Huang CP, Lu J, Seon H, Lee AP, Flanagan LA, Kim HY, Putnam AJ, Jeon NL. Engineering microscale cellular niches for three-dimensional multicellular co-cultures. Lab on a Chip. 2009; 9(12):1740–1748. [PubMed: 19495458]

26. Kim MS, Yeon JH, Park JK. A microfluidic platform for 3-dimensional cell culture and cell-based assays. Biomedical Microdevices. 2007; 9(1):25–34. [PubMed: 17103048]

27. Walker GM, Beebe DJ. A passive pumping method for microfluidic devices. Lab on a Chip. 2002; 2(3):131–134. [PubMed: 15100822]

28. Warrick JW, Murphy WL, Beebe DJ. Screening the Cellular Microenvironment: A Role for Microfluidics. Biomedical Engineering, IEEE Reviews in. 2008; 1:75–93.

29. Meyvantsson I, Warrick JW, Hayes S, Skoien A, Beebe DJ. Automated cell culture in high density tubeless microfluidic device arrays. Lab on a Chip. 2008; 8(5):717–724. [PubMed: 18432341]

30. Puccinelli JP, Su X, Beebe DJ. Automated high-throughput microchannel assays for cell biology: Operational optimization and characterization. JALA Charlottesv Va. 15(1):25–32. [PubMed: 20209121]

31. Sung KE, Su G, Pehlke C, Trier SM, Eliceiri KW, Keely PJ, Friedl A, Beebe DJ. Control of 3-dimensional collagen matrix polymerization for reproducible human mammary fibroblast cell culture in microfluidic devices. Biomaterials. 2009; 30(27):4833–4841. [PubMed: 19540580]

32. Meyvantsson I, Beebe DJ. Cell Culture Models in Microfluidic Systems. Annual Review of Analytical Chemistry. 2008; 1:423–449.

33. Rhee S, Grinnell F. Fibroblast mechanics in 3D collagen matrices. Advanced Drug Delivery Reviews. 2007; 59(13):1299–1305. [PubMed: 17825456]

34. Bauer M, Su G, Beebe DJ, Friedl A. 3D microchannel co-culture: method and biological validation. Integrative Biology. 2(7–8):371–378.

35. Kuperwasser C, Chavarria T, Wu M, Magrane G, Gray JW, Carey L, Richardson A, Weinberg RA. Reconstruction of functionally normal and malignant human breast tissues in mice. Proceedings of the National Academy of Sciences of the United States of America. 2004; 101(14):4966–4971. [PubMed: 15051869]

36. Su G, Blaine SA, Qiao DH, Friedl A. Shedding of syndecan-1 by stromal fibroblasts stimulates human breast cancer cell proliferation via FGF2 activation. Journal of Biological Chemistry. 2007; 282(20):14906–14915. [PubMed: 17344212]

37. Xie Y, Wang F, Puscheck EE, Rappolee DA. Pipetting causes shear stress and elevation of phosphorylated stress-activated protein kinase/jun kinase in preimplantation embryos. Molecular Reproduction and Development. 2007; 74(10):1287–1294. [PubMed: 17492777]
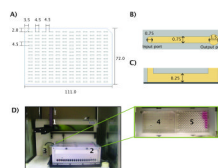
Figure 1. Microchannel dimensions and the automated platform
A) Geometry of a microchannel array composed of 192 channels used in the automated platform. B) Top view of a single microchannel showing the input (left) and output (right) ports. C) Side view of a single microchannel mounted on a polystyrene omnitray (dark gray). D) The automated microfluidic platform and its components showing: 1) dispensing pipette, 2) Peltier device (for temperature control), 3) waste reservoir, and a top view of Peltier device showing: 4) microchannel array, and 5) 96 well plate reservoir containing media and collagen/cell suspension. Dimensions in mm.

Figure 2. Diagram of automated processes
Three main processes were performed by the automated platform after the system was optimized. Colored squares represent separate loops. SF= serum free, IP=input port, OP= output port, RT= room temperature.
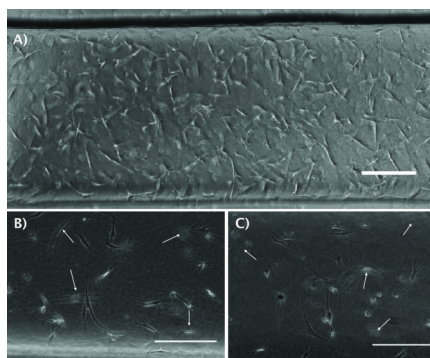
Figure 3. Morphology and distribution of HMFs cells loaded manually and with the automated platform
A) Phase contrast image of Human Mammary fibroblasts (HMFs) loaded inside a microchannel with 1.3 mg/mL type-I collagen using the automated platform. Cells inside a microchannel loaded B) by hand, and C) with the automated platform show similar morphology. Arrows point fibroblasts in different focal planes, suggesting a 3D distribution. Scale bars represent 200 µm.
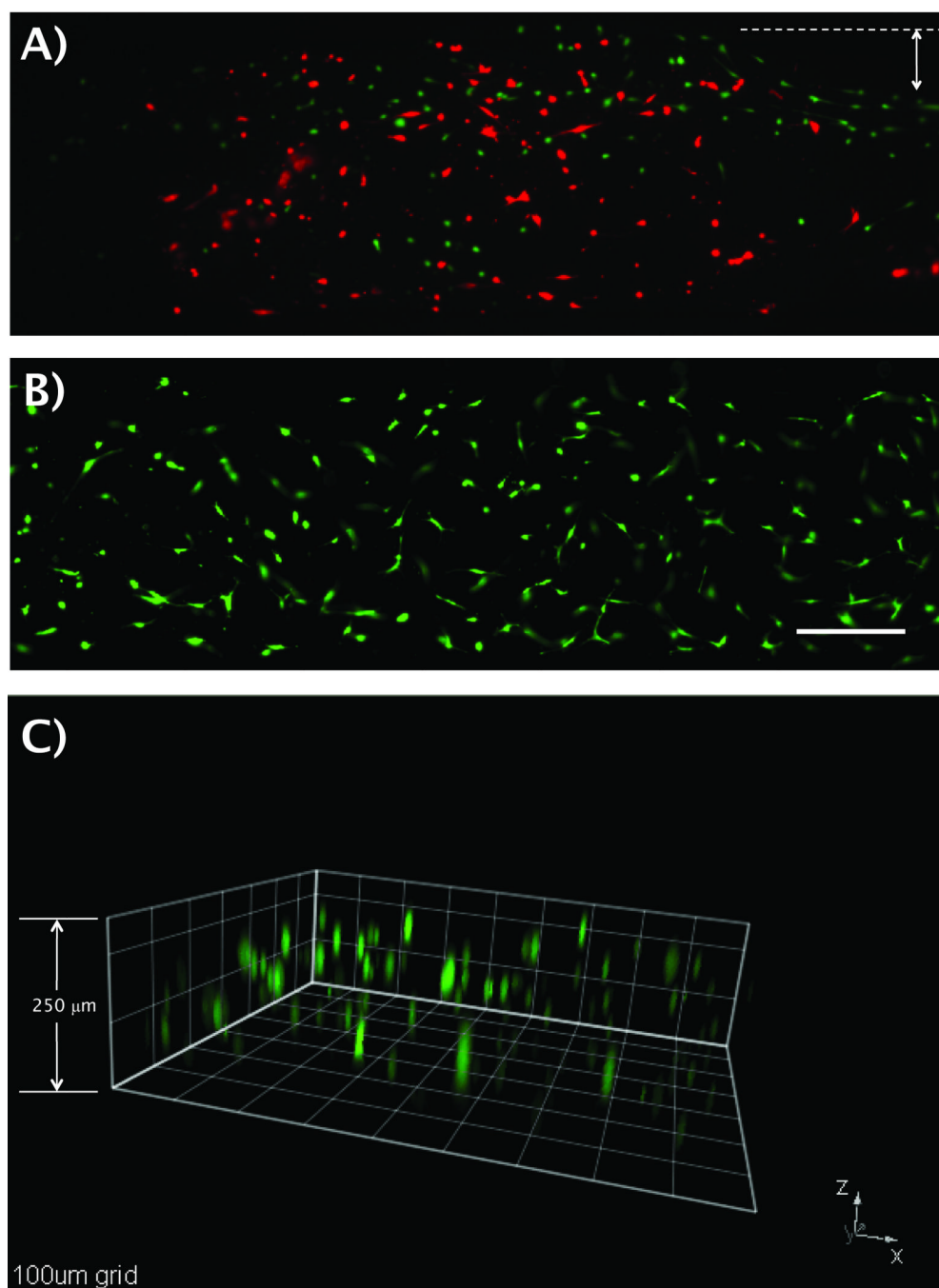
Figure 4. Viability and three-dimensional distribution of HMFs cells loaded with the automated platform

Fluorescent images of HMFs suspended in 1.3mg/mL type-I collagen, loaded and stained with the automated platform A) before, and B) after system optimization. A) A cell viability of 31% and collagen contraction on the sides of the microchannel was observed before system optimization. B) A viability of 99% and minimum collagen contraction was found after the system was optimized. Calcein AM stained for live cells (green) and Ethidium homodimer-1 for dead cells (red). Arrow shows collagen contraction before system optimization. C) A 250μm high microchannel was loaded with HMFs using the automated

platform. HMFs cells (green) showed a 3D distribution along 200µm of type-I collagen matrix. Squares dimensions are 100µm. Scale bar represents 200 µm.
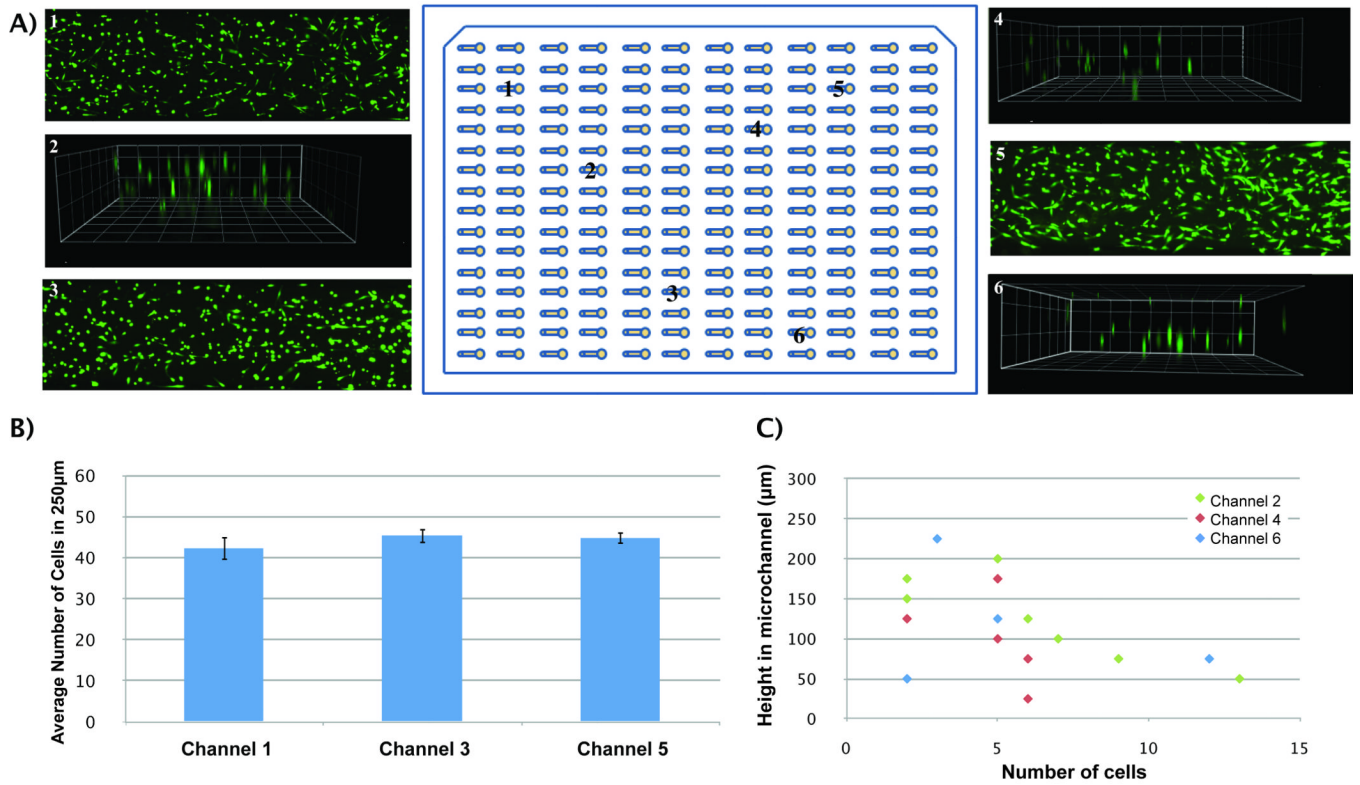
Figure 5. Uniformity in viability and 3D distribution of cells in the MCA
A) Microchannels 1, 3 and 5 show cells with an average viability of 90%. Channels 2, 4 and 6 show a 3-dimensional distribution of cells inside 250µm high microchannels. B) Average number of HMFs along 250µm sections of microchannels 1, 3 and 5 show no significant differences among these channels. C) HMFs are distributed in 3D along different heights in microchannels 2, 4 and 6. Squares dimensions are 100µm.
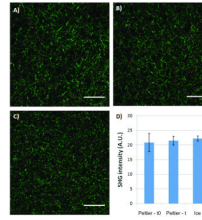
Figure 6. Collagen fiber polymerization in microchannels loaded on Peltier device and over ice
Second Harmonic Generation (SHG) images of microchannels loaded with type-I collagen
on Peltier device A) before starting the cell seeding process (0 minutes, Process 2), and B)
after the duration of cell seeding process (22 minutes, Process 2). A similar type-I collagen
fiber structure was observed in C) microchannel loaded using traditional preparation
methods over ice, thus confirming proper fiber collagen polymerization in microchannels
loaded on the Peltier device. D) No significant differences in SHG intensity were found for
microchannels loaded on Peltier device before (Peltier-t0) or after the cell seeding process
(Peltier-t) or when samples were kept over ice (Ice). A.U. measured as arbitrary units. Scale
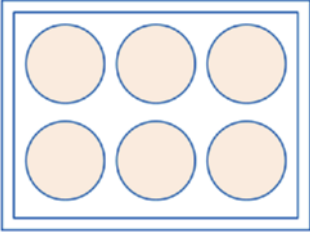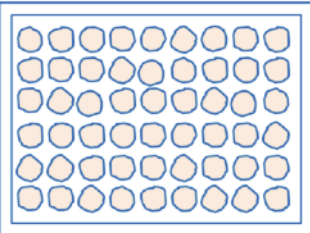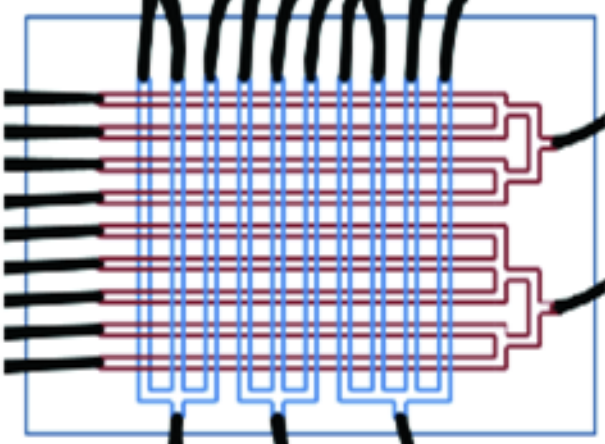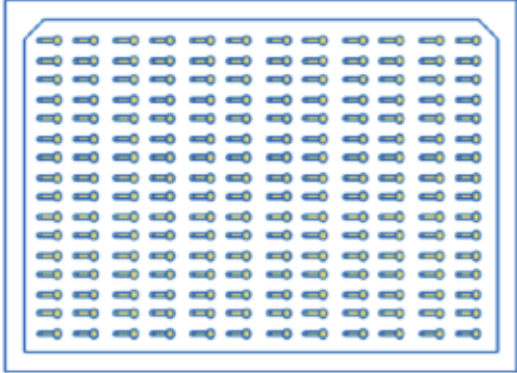bars represent 50µm.
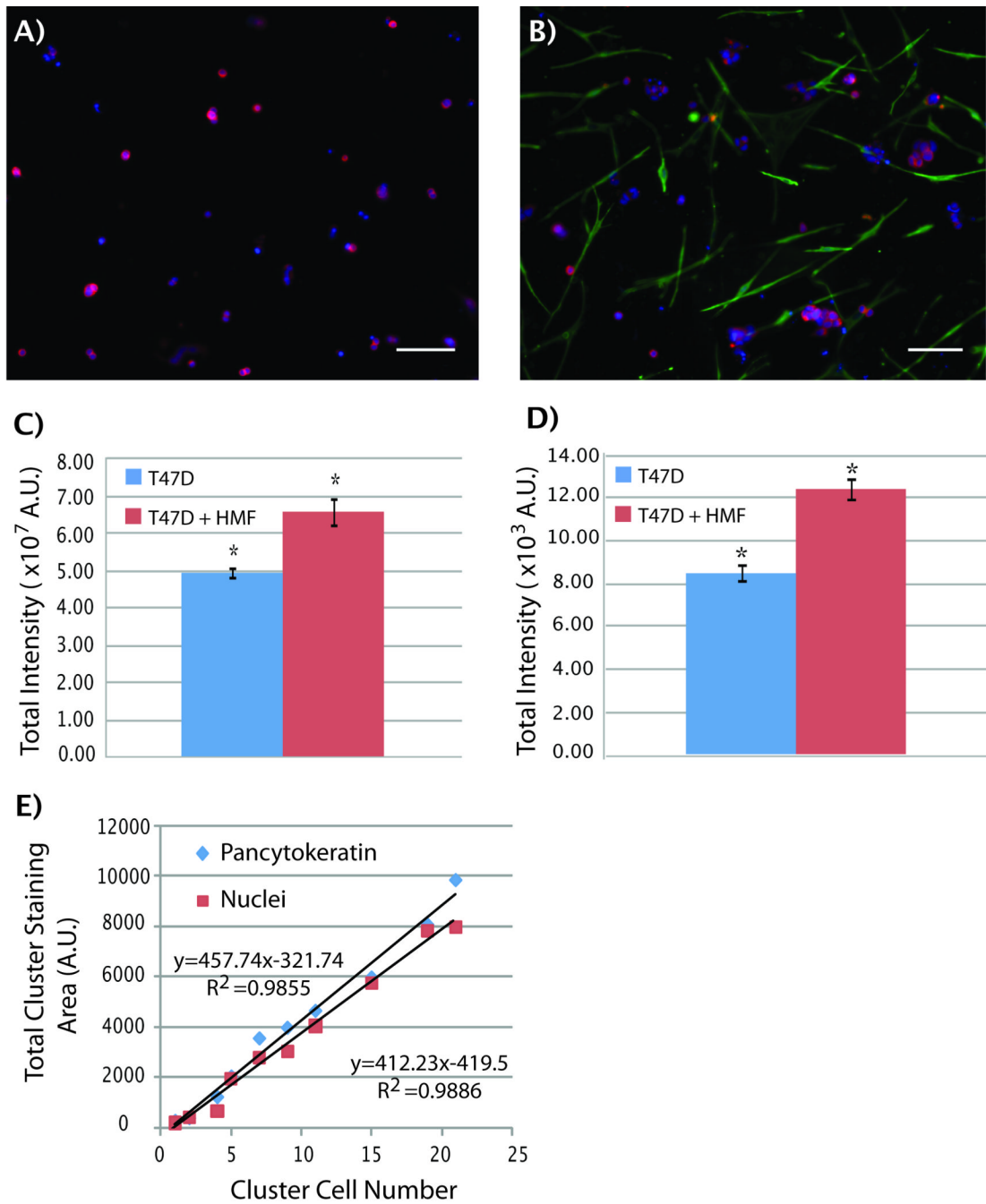
Figure 7. Screening of T47D cell growth

T47D cells were grown for five days and stained for pancytokeratin (CK), vimentin (green) and cell nuclei (Hoechst). A) T47D carcinoma cells grow into small, irregular clusters in monocultures. B) In contrast, in presence of HMFs cells, T47D cells grow into bigger clusters. C) A pancytokeratin total area analysis was performed via fluorescent scanning and total fluorescence intensity in microchannels showed a 1.5-fold increase in co-cultures (red bar) when compared to monocultures (blue bar). D) Manual calculation of total nuclei staining area also shows a 1.5-fold increase in T47D growth in co-cultures. E) A linear correlation was found between the number of T47D cells in the clusters and the total CK-

positive (blue diamond) and nuclei staining (red squares) areas. Scale bars represent 150µm. n=30, * p<0.02. A.U. measured as arbitrary units.

Table 1

Advantages and limitations of currently available screening methods for 3D cell culture.

Method	Array Format	Advantages	Limitations
Traditional 3D cell culture assays	**Well plates**	**1** Mimics *in vivo* conditions better than 2D cell culture models **2** Only requires a pipette for manipulating fluids.	**1** Cells suspe... ECM prote... settle to the... of wells **2** Uses relativ... volumes of... (200–500µ... **3** Limited thr...
Cellular microarrays	**Patterned substrates**	**1** Higher-throughput analysis of cell-matrix, cell-cell interactions or toxicity screenings than with traditional 3D cell culture assays **2** Reduced amount of reagents (3–40µL)	**1** Cells are cu... top of patte... surfaces **2** Inhomogen... and sample... can occur w... spotting sa... **3** Entire patte... substrate is... to the same... stimuli, wh... increases th... potential of... between sp... **4** Requires op... robotic spo...
Microfluidic valved arrays	**Valved microchannels**	**1** Allows the incorporation of multiple fluids and cell types. **2** Compatible for 2D and 3D cell cultures. **3** Reduced amount of reagents (0.1–1.5µL/min)	**1** 3D matrix o... the network... **2** Uses compl... connections... pumps **3** Low compartme... limits its incorporati... automated l... handles (A... **4** A significan... of reagents... dead volum...

Method	Array Format	Advantages	Limitations
Tubeless microfluidic devices	**Tubeless microchannels** _(array format diagram)_	**1** Passive pumping does not require pumps or connectors and enables its incorporation with automated liquid handles **2** Enclosed channels can be treated individually with different soluble formulations **3** Compatible for 2D and 3D culture **4** Reduced amount of reagents (2–5µL)	**1** Longer pro... required fo... individualiz... treatment